Low-temperature sintering, dielectric performance, and far-IR reflectivity spectrum of a lightweight $NaCaVO_4$ with good chemical compatibility with silver

Ying Xiong[2], Zhuo Xing[1*], Juhai Weng[1], Chi Ma[1], Jibran Khaliq[4], Chunchun Li[2, 3*]

[1]*School of Electronic Information Engineering, Xijing University, Xi'an 710123, China*

[2]*College of Information Science and Engineering, Guilin University of Technology, Guilin, 541004, China*

[3]*School of Materials Science and Engineering, Nanchang University, Nanchang, 330031, People's Republic of China*

[4]*Department of Mechanical and Construction Engineering, Faculty of Engineering and Environment, Northumbria University at Newcastle, NE1 8ST, UK*

Abstract

As one of the candidates of low-temperature cofired ceramics (LTCC), the sintering behavior, dielectric properties, and silver chemical compatibility of $NaCaVO_4$ were studied. The bulk ceramic samples were densified well at a low sintering temperature of 720 °C with an optimal bulk density of 2.87 g/cm^3. Excellent microwave dielectric properties with a low relative permittivity ε_r ~ 9.9, a high quality factor $Q\times f$ ~ 31,600 GHz, and a temperature coefficient of resonance frequency τ_f ~ -66.5 ppm/°C were achieved at 11.5 GHz. The far infrared reflectivity spectra revealed the intrinsic dielectric properties (relative permittivity of 8.34 and dielectric loss of 2.7×10^{-4}) are comparable to the measured values. The absence of chemical reaction between $NaCaVO_4$ and silver at firing temperature, evidenced by X-ray diffraction and energy dispersive spectroscopy indicated the potential prospect for LTCC application. Furthermore, the very low density of $NaCaVO_4$ opens up an avenue for its potential applications in light-weight devices.

Keywords: Low-density materials; Ceramics; Sintering behavior; Dielectric properties; Microwave band

* Authors to whom correspondence should be addressed: xingzhuo@xijing.edu.cn; lichunchun2003@126.com

1. Introduction

Recent advances in the fifth generation (5G) mobile communication, internet of things (IoT) and wireless local area networks (WLAN) point towards the development of electronic terminals with specific focus on miniaturization, multifunctionality, and light-weight [1-3]. As permittivity is inversely related to device size, high-permittivity materials has been recognized as an effective method to realize miniaturization [1, 4]. However, such high-permittivity dielectrics usually exhibit high dielectric loss and inferior thermal stability resulting in loss/degradation of dielectric properties, keeping the potential options very limited [5, 6]. Low-temperature cofired ceramic (LTCC) is an alternative technology for device miniaturization due to its potential packaging of dielectrics with conductors and embedding passive components [7]. The most important requirement for dielectrics in LTCC is the suitable densification temperature and comparable chemical and thermal expansion characteristics with the electrode materials (e.g. silver).

In the last decade, two main strategies have been proposed to explore low-firing ceramics:

(i): Altering the synthesis and compositional parameters of well-developed materials (e.g. $BaTi_4O_9$, $Ba_2Ti_9O_{20}$, and $Mg_5Nb_4O_{15}$) with prominent dielectric performances such as:

(a):by adding low-melting-point oxides or glasses,

(b): chemical synthesis, or

(c): applying ultrafine powders to effectively lower their sintering temperatures [8-10];

or

(ii): developing novel dielectrics that can be densified intrinsically at low temperatures without additional sintering aids[11, 12].

The latter is a more desirable technique compared to the first one due to the simple processing

and comprehensive dielectric properties. The intensively explored low-sintering materials mainly include Li_2O, Bi_2O_3, TeO_2, MoO_3, WO_3, and V_2O_5 [13-19]. Recently, vanadates have attracted considerable attention for their potential applications in LTCC in consideration of their low molten point and outstanding microwave dielectric properties [20-24]. For example, Yao *et. al* reported that $Ca_5Mn_4(VO_4)_6$ ceramic sintered at 875 ^oC exhibited good microwave properties $\varepsilon_r \sim 11.2$, $Q \times f \sim 33{,}800$ GHz, and $\tau_f \sim -70$ ppm/°C [23]. Moreover, $NaCa_4V_5O_{17}$ ceramic sintered at 840 °C has a high $Q \times f \sim 51{,}000$ GHz but low $\varepsilon_r \sim 9.72$ [24].

$NaCaVO_4$ which is a double vanadate, adopts an orthorhombic structure with a space group *Cmcm*, isomorphous with Na_2CrO_4 [25]. Previous work of $NaCaVO_4$ mainly focused on its luminescence properties, and it has been recognized as a promising host for rare-earth activators to enhance luminescence yield [26]. One of the most important characteristics of $NaCaVO_4$ is the extremely low synthesis temperature which is around 700 ^oC [27] which ultimately predicts the optimal sintering temperature of $NaCaVO_4$ to be low. Despite these properties, no attempts have been made to probe the dielectric properties of $NaCaVO_4$ to the best of our knowledge. Therefore, in this work, dense $NaCaVO_4$ ceramic was fabricated via simple oxide mixing route to develop novel low-firing microwave dielectric ceramics. The sintering behavior and structure stability were evaluated in a wide temperature range (640-740 ^oC) and dielectric properties at microwave frequency bands were characterized.

2. Experimental procedure

Synthesis: Polycrystalline $NaCaVO_4$ ceramics were fabricated by a mixed oxide route using starting materials (all have purity > 99.9%, Guo-Yao Co. Ltd, China) of Na_2CO_3, $CaCO_3$, and NH_4VO_3. The starting materials were weighed stoichiometrically and wet ball-milled for 4 h using zirconia balls.

The dried mixture was calcined at 600 °C for 4 h to obtain pure $NaCaVO_4$ phase. Then the calcined powders were crushed and re-milled, followed by addition of PVA binders. Finally, the obtained powders were pressed into pellets and fired to 550 °C for 2 h to remove PVA, and then sintered in the temperature range from 660 to 740 °C for 6 h.

Characterization: X-ray diffractometer (Cu*Kα1*, 1.54059 Å, Model X'Pert PRO, PANalytical, Almelo, Holland) was employed to identify the crystal structure of the calcined powders and bulk ceramics. The bulk density was evaluated via Archimede's method. The surfaces of bulk ceramic samples were initially polished and thermally etched at lower than their optimal sintering temperature for 30 min. The microstructures were observed using a scanning electron microscope (Model JSM6380-LV SEM, JEOL, Tokyo, Japan), while Oxford X-Max microanalysis system (EDX) was used for elemental analysis. The room-temperature infrared reflectivity spectra were measured by a Bruker IFS 66v FT-IR spectrometer (Bruker Optics, Ettlingen, Germany). The relative permittivity and quality factor at microwave frequency bands were measured based on the Hakki and Coleman method [28] using a network analyzer (Model N5230A, Agilent Co., Palo Alto, Canada). The thermal shift (τ_f) of the resonance frequency was monitored in the temperature range of T_1 (25 °C) to T_2 (85 °C) inside a temperature chamber (Delta 9039, Delta Design, San Diego, CA), and calculated by Eq. (1):

$$\tau_f = \frac{f_2 - f_1}{f_1(T_2 - T_1)} \qquad (1)$$

where f_1 and f_2 are the corresponding resonance frequency at T_1 and T_2, respectively.

3. Results and discussion

To get a clear perspective of the chemical reactions and their temperatures of the starting materials, thermal analysis through thermo-gravimetry (TG) and differential scanning calorimetry (DSC) was conducted on initially mixed raw materials. A total mass loss of ~ 23.3% is detected based on the TG

curve as shown in Figure 1a. The mass loss occurred at two different temperature, a mass loss of 6.74% occurred at a lower temperature range (< 400 ^{o}C), while a more pronounced mass loss (16.5%) took place in the temperature of 400 ^{o}C to 600 ^{o}C accompanied by a broad exothermic peak (~ 450 ^{o}C) in the DSC curve. Previous work demonstrates NH_4VO_3 gradually decomposes into NH_3, H_2O, and V_2O_5 at nearly 370 ^{o}C [24]. The theoretical thermal decomposition mass loss of NH_4VO_3 was nearly 9.62% in the present system, which is much higher than the measured value (6.74%), suggesting that NH_4VO_3 does not decompose completely. According to the chemical reaction [$2NH_4VO_3 + Na_2CO_3 + 2CaCO_3 = 2NaCaVO_4 + 2NH_3 (\uparrow) + H_2O (\uparrow) + CO_2 (\uparrow)$], the theoretical mass loss was calculated to be 17.8% in total, which is lower than the measured value (~ 23.3%). Thus, it is concluded that the volatilization of absorbed moisture during mixing and the partial decomposition of NH_4VO_3 was responsible for the first-step mass loss (below 400 ^{o}C), while the subsequent more pronounced mass loss (in the temperature of 400 ^{o}C to 600 ^{o}C) was caused by the decomposition of NH_4VO_3 and carbonates. Moreover, DSC curve exhibited an exothermic peak at 450 ^{o}C revealed the chemical reaction to form the $NaCaVO_4$ phase.

To identify the phase structure and stability, the room-temperature XRD patterns were recorded on the calcined powders at selected temperatures (660 - 740 ^{o}C for 6 h) as shown in Figure 1b. By indexing with the standard JCPDS No. 75-2310, an orthorhombic structure with a space group *Cmcm* was confirmed. Over the whole temperature range, no obvious difference in the XRD patterns was found, indicating the thermal stability of the phase structure.

The Rietveld refinement was performed on the $NaCaVO_4$ powder sintered at 700 ^{o}C using Fullprof software to understand the fine structure of $NaCaVO_4$. The fitting *R* factors were R_{wp} = 11.93%, R_p = 10.02% respectively and indicated that the refinement results were reliable as shown in Figure 1c.

The lattice parameters were calculated to be a = 5.8690(1) Å, b = 9.2999(3) Å, c = 7.1561(3) Å, while volume of the cell (V) was calculated to be 390.5926(5) Å^3, respectively. A schematic of the $NaCaVO_4$ structure is presented in the inset of Figure 1d. Ca can be seen located at the center of oxygen octahedron (Wyckoff position: 4b) while both Na and V atoms are located at the center of oxygen tetrahedron (Wyckoff position 4c). The neighboring Ca octahedron are connected through sharing edges to form the layers parallel to the (001) plane. Both NaO_4 and VO_4 tetrahedra are linked to CaO_6 octahedron through corner-linking. Two sets of bond lengths for Na-O in NaO_4 tetrahedra and V-O in VO_4 tetrahedra were calculated, Na-O bond-lengths were 2.4738 Å and 2.3166 Å, while for V-O, the bond lengths were 1.6003 Å and 1.7341 Å respectively. Moreoever, the distortion degree of the tetrahedra can be estimated via the equation [29]:

$$\text{Polyhedron distortion} = \frac{(largest - smallest)\ M-O_{distance}}{average\ M-O_{distance}} \qquad (2)$$

where M denotes the cations in a polyhedron and O denotes the bonded oxygen in the same polyhedron. The calculated distortion degree was ~ 6.56% and ~ 2.55% for NaO_4 and VO_4, respectively. The distortion difference is related to the different ionic radius and electrovalence for Na^+ (0.99 Å, C.N. = 4) and V^{5+} (0.355 Å, C.N. = 4). It is speculated that such an off-center location for Na and V in tetrahedra will enhance the local polarization and consequently will improve the dielectric properties.

It is well accepted that the electrical properties of microwave ceramics critically depend on several parameters, especially, the optimum dielectric performances are generally observed in ceramics exhibiting the highest density (compared to theoretical density of the bulk ceramic) [230, 31]. Thus, the sintering behavior of the $NaCaVO_4$ ceramics was studied in terms of microstructural and density variation as a result of different sintering temperature. As demonstrated in Figure 2 (a-e), the porosity of the ceramics reduced along with visible grain growth with the increasing sintering temperature. A

relatively dense microstructure with closely packed grains could be obtained for a sintering temperature of 720 °C. The variation in bulk and relative densities as functions of sintering temperature are shown in Figure 2f. The sample sintered at 660 °C showed a porous microstructure. The bulk density of the sample was 2.68 g/cm^3, which is only 88.4% of the theoretical value (3.03 g/cm^3). As the sintering temperature increased, the density gradually increased to a maximum value of 2.87 g/cm^3 (~ 94.6% for relative density). These results clearly point towards and additional benefit of $NaCaVO_4$ compared to most commercial microwave ceramics in terms of the density. The density of present $NaCaVO_4$ ceramics is nearly half of the commercially known microwave ceramics, which makes $NaCaVO_4$ superior in light-weight devices.

The variations in microwave dielectric properties (ε_r, $Q\times f$, and τ_f) as a function of sintering temperature are shown in Figure 3. An obvious correlation between relative permittivity and sintering temperature could be seen. The relative permittivity increased initially followed by a decrease, yielding the maximum value of 9.9 at 720 °C. A similar variation was also seen for the quality factor. The maximum value of 31,600 GHz corresponds to a sintering temperature of 720 °C. As a result, the densest sample of all possessed the optimal relative permittivity and quality factor, which is consistent with the previous work [11]. Such correlation for ε_r and $Q\times f$ on density revealed the predominant effects of bulk density on dielectric behavior. Figure 3a also shows the porosity corrected relative permittivity (ε_{corr}) calculated through the Bosman and Having's equation [$\varepsilon_{corr} = \varepsilon_r (1 + 1.5p)$ where p is the fractional porosity] [32]. The calculated ε_{corr} values were slightly higher than the measured values, further confirming the significant influence of density on dielectric properties. Besides, it should be noted a large deviation (Δ = 25%) between the calculated relative permittivity of $NaCaVO_4$ by the Clausius-Mossotti theory [33] (ε_r = 7.45) and the measured value (ε_r = 9.9). Such deviation is the result

of contribution of the off-center ions in NaO_4 and VO_4 tetrahedra to the local polarization (6.56%), which is consistent with Shannon′s theory [33]. On the contrary, the τ_f value of $NaCaVO_4$ exhibited a weak dependence on the sintering temperature and fluctuated around -60 ppm/ºC. the τ_f value is sensitive to phase transition and coexistence phases [24]. The fact that no phase transition or the second phase emerged over the temperature range (660-740 ºC) accounts for the weak dependence of the .

The infrared reflection spectra (IR) are mainly caused by the absorption of the polar lattice vibration and can be used to study the intrinsic microwave dielectric properties. As shown in Figure 4, the infrared reflectivity spectra of $NaCaVO_4$ ceramic is shown. Based on the classical oscillator model, the infrared reflectivity $R(\omega)$ can be obtained from the complex dielectric function $\varepsilon^*(\omega)$ which can be calculated from the following equations [34, 35]:

$$R(\omega) = \left| \frac{\sqrt{\varepsilon^*(\omega)} - 1}{\sqrt{\varepsilon^*(\omega)} + 1} \right|^2 \tag{3}$$

$$\begin{aligned} \varepsilon^*(\omega) &= \varepsilon_\infty + \sum_{j=1}^{n} \frac{S_j(\omega_j^2 - \omega^2)}{(\omega_j^2 - \omega^2)^2 + \omega^2\gamma^2} - i\sum_{j=1}^{n} \frac{S_j\omega\gamma_j}{(\omega_j^2 - \omega^2)^2 + \omega^2\gamma^2} \\ &= \varepsilon'(\omega) - i\varepsilon''(\omega) \end{aligned} \tag{4}$$

$$\tan\delta = \frac{\varepsilon''}{\varepsilon'} = \sum_{j=1}^{n} \frac{S_j\omega\gamma_j}{\varepsilon'(\omega)\omega_j^4} \tag{5}$$

where n represents the order of transverse polar-phonon modes; ω_j, S_j, and j_γ is the frequency, strength, and damping constant of the j-th mode; and ε_∞ is the relative permittivity caused by electronic polarization.

According to the factor group analysis of orthorhombic structure with a space group *Cmcm*, the IR active mode of $NaCaVO_4$ has been confirmed to be $6B_{1u}+7B_{2u}+5B_{3u}$ [36]. As shown in Table 1, 14 IR active modes were adopted to fit the IR reflectivity spectra. Figure 4a shows the measured and calculated IR spectra and Figure 4b shows the real and imaginary parts of the complex responses

obtained from the fitting of the IR reflectivity spectra. The calculated permittivity and dielectric loss at the microwave range were 8.34 and 2.7×10^{-4}, 42,500 GHz, respectively. The measured permittivity (9.9) was slightly higher than the calculated value which could be attribute to the higher frequencies at IR spectra compared to the microwave range. The extrinsic dielectric contributions were gradually withdrawn with the increasing frequency. However, the calculated dielectric loss had the same order of magnitude as the measured one, indicating that the absorptions of structural phonon oscillation at the infrared were dominated by the dielectric loss at the microwave range.

For LTCC processing, dielectric ceramic layers and metallic electrode layers such as silver were stacked alternatively. The outstanding chemical compatibility of ceramic with electrode (silver in this case) is essential, especially, when they were cofired at elevated temperatures [7, 39, 40]. Figure 5a shows the X-ray diffraction patterns of the cofired $NaCaVO_4$ ceramic with 20 wt.% Ag at 720 ^oC. Comparing with the standard PDF card for $NaCaVO_4$ (No. 75-2310) and silver (No. 87-0719), no additional XRD peaks could be observed. It suggests that no chemical reaction between $NaCaVO_4$ and silver took place during cofiring. Backscattered electron image (BSEM) provided another evidence for chemical compatibility between them in Figure 5b. It demonstrated a clear separation of silver grains (the big gray ones, as confirmed by the EDS) from the ceramic matrix. The prominent chemical compatibility with the silver electrode implies $NaCaVO_4$ a promising candidate for LTCC.

Table 2 lists sintering temperature and microwave dielectric properties of several vanadates [12, 24, 37, 38]. All vanadates have relatively low sintering temperature (< 960 ^oC) and chemical compatibility with silver, suggesting their promising prospect in LTCC technology. Amongst them, the Bi-containing compounds having high or moderate relative permittivity are related to their lone pair electron feature. In contrast, low permittivity was achieved in the sample composed of rich alkali

metals with particular interest in Na-based vanadates that showed the lowest density (e.g. 2.87 g/cm^3 for $NaCaVO_4$) compared to commercially known microwave ceramics.

Conclusions

The low-density $NaCaVO_4$ ceramic was fabricated by a simple mixing oxide route at low temperatures. Thermal analysis reveals the phase formation of $NaCaVO_4$ at a very low temperature of ~ 450 ^oC, and exhibited thermal phase stability within a temperature span of 640-740 ^oC. The Rietveld refinement confirmed that $NaCaVO_4$ adopted an orthorhombic structure with a space group *Cmcm*. The sintering behavior and dielectric performances were optimized based on their variation in sintering temperatures. The ceramic sintered at 720 ^oC possessed a bulk density of 2.87 g/cm^3 and enhanced microwave dielectric properties $\varepsilon_r \sim 9.9$, $Q \times f \sim 31{,}600$ GHz, and $\tau_f \sim$ -60 ppm/^oC,316,00 GHz. Besides, far-infrared spectra analysis reveal the optimum quality factor of $NaCaVO_4$ cramics with 42,500 GHz and offer the possibility to further improve their dielectric properties. $NaCaVO_4$ showed no chemical reaction with silver for cofiring at 720 ^oC. As a result, the lightweight, low sintering temperature, comparable dielectric properties, and chemical compatibility with silver electrodes indicated the potential application of $NaCaVO_4$ in LTCC technology.

Acknowledgments

Chunchun Li gratefully acknowledges the financial support from the Natural Science Foundation of China (No. 62061011) and the Natural Science Foundation of Guangxi Zhuang Autonomous Region (No. 2018GXNSFAA281253, 2019GXNSFGA245006).

Conflict of interest statement

No conflict of interest exists in the submission of this manuscript, and the manuscript is approved by all authors for publication. I would like to declare on behalf of my co-authors that the work

described was original research that has not been published previously, and not under consideration for publication elsewhere, in whole or in part.

References

[1] M.T. Sebastian, Dielectric materials for wireless communication, Elsevier Publishers, Oxford, U.K. 2008.

[2] B. Ullah, W. Lei, Y.F. Yao, X.C. Wang, X.H. Wang, M.U. Rahman, W.Z. Lu, Structure and synergy performance of (1-x)$Sr_{0.25}Ce_{0.5}TiO_3$-xLa$(Mg_{0.5}Ti_{0.5})O_3$ based microwave dielectric ceramics for 5G architecture, J. Alloys Compd., 763 (2018) 990-996.

[3] Q. Lin, K. Song, B. Liu, H.B. Bafrooei, D. Zhou, W. Su, F. Shi, D. Wang, H. Lin, I.M.Reaney, Vibrational spectroscopy and microwave dielectric properties of $AY_2Si_3O_{10}$ (A = Sr, Ba) ceramics for 5G applications, Ceram. Int., 46 (2020) 1171-1177.

[4] Y. Zhang, S.H. Ding, C. Li, T.X. Song, Y.C. Zhang, Bond analysis of novel $MnZrTa_2O_8$ microwave dielectric ceramics with monoclinic structure, J. Mater. Sci., 55 (2020) 8491-8501.

[5] L.X. Pang, D. Zhou, D.W. Wang, J.X. Zhao, W.G. Liu, Z.X. Yue, I.M. Reaney, Temperature stable $K_{0.5}(Nd_{1-x}Bi_x)_{0.5}MoO_4$ microwave dielectrics ceramics with ultra-low sintering temperature, J. Am. Ceram. Soc., 101 (2018) 1806-1810.

[6] H.S. Park, K.H.Yoon, Relationship between the bond valence and the temperature coefficient of the resonant frequency in the complex perovskite $(Pb_{1-x}Ca_x)[Fe_{0.5}(Nb_{1-y}Ta_y)_{0.5}]O_3$, J. Am. Ceram. Soc., 84 (2001) 99-103.

[7] M.T. Sebastian, H. Jantunen, Low loss dielectric materials for LTCC applications: a review, Int. Mater. Rev., 53 (2008) 57-90.

[8] D.W. Kim, D.G. Lee, K.S. Hong, Low-temperature firing and microwave dielectric properties of $BaTi_4O_9$ with Zn-B-O glass system, Mater. Res. Bull. 36 (2001) 585-595.

[9] C.L. Huang, M.H. Weng, C.T. lion, C.C. Wu, Low-temperature sintering and microwave dielectric properties of $Ba_2Ti_9O_{20}$ ceramics using glass additions, Mater. Res. Bull. 35 (2000) 2445-2456.

[10] H.T. Wu, Q.J. Mei, Effects of B_2O_3 addition on sintering behavior and microwave dielectric properties of $Mg_5Nb_4O_{15}$ ceramics prepared by the sol-gel method, J. Alloys Compd., 651 (2015) 393-398.

[11] H.H. Guo, D. Zhou, L.X. Pang, Z.M. Qi, Microwave dielectric properties of low firing temperature stable scheelite structured (Ca, Bi)(Mo, V)O_4 solid solution ceramics for LTCC applications, J. Eur. Ceram. Soc., 39 (2019) 2365-2373.

[12] X.Q. Chen, H. Li, P.C. Zhang, G.S. Li, Microwave dielectric properties of $Co_2P_2O_7$ ceramics, Ceram. Int., 47 (2021) 1980-1985.

[13] C. Z. Yin, H.C. Xiang, C.C. Li, H. Porwal, L. Fang, Low-temperature sintering and thermal stability of Li_2GeO_3-based microwave dielectric ceramics with low permittivity, J. Am. Ceram. Soc., 101 (2018) 4608-4614.

[14] E.K. Suresh, R. Ratheesh, Structure and microwave dielectric properties of glass-free low-temperature co-friable $SrMV_2O_7$ (M = Mg, Zn) ceramics, J. Alloys Compd., 808 (2019) 151641.

[15] G. Subodh, M.T. Sebastian, Glass-free $Zn_2Te_3O_8$ microwave ceramic for LTCC applications, J. Am. Ceram. Soc., 90 (2007) 2266-2268.

[16] Z. Xing, C.J. Shen, C.Z. Yin, H.J. Ye, C.C. Li, Low-temperature synthesis and dielectric characterization of $La_2Mo_2O_9$ ceramic at RF and microwave frequencies, Adv. Appl. Ceram., (2020) 1-6.

[17] H.C. Yang, S.R. Zhang, H.Y. Yang, Y. Yuan, E.Z. Li, $Gd_2Zr_3(MoO_4)_9$ microwave dielectric ceramics with trigonal structure for LTCC application, J. Am. Ceram. Soc., 103 (2020) 1131-1139.

[18] B. Li, W. Liu, H.S. Leng, Effect of non-stoichiometry on the microstructure and microwave dielectric properties of $Ca_5Mg_{4+x}V_6O_{24}$ ($-0.05 \le x \le 0.15$) ceramics, J. Mater. Sci., 55 (2020) 3795-3802.

[19] K. Cheng, C.C. Li, C.Z. Yin, Y. Tang, Y.H. Sun, L. Fang, Effects of Sr^{2+} substitution on the crystal structure, Raman spectra, bond valence and microwave dielectric properties of $Ba_{3-x}Sr_x(VO_4)_2$ solid solutions, J. Eur. Ceram. Soc., 39 (2019) 3738-3743.

[20] A. Pirvaram, E.T. Nassaj, H.T. Armaki, W.Z. Lu, W. Lei, H.B. Bafrooei, Study on structure, microstructure and microwave dielectric characteristics of CaV_2O_6 and $(Ca_{0.95}M_{0.05})V_2O_6$ (M = Zn, Ba) ceramics, J. Am. Ceram. Soc., 102

(2019) 5213-5222.

[21] G.J. Yang, C.Z. Yin, Y.C. Li, Y.P. Kang, S.H. Zhang, C.C. Li, Improvement in thermal stability of resonance frequency of $LiCa_3MgV_3O_{12}$ ceramics through compositional modulation, J. Mater. Sci. - Mater. Electron., 31 (2020) 10605-10611.

[22] D. Zhou, L.X. Pang, J. Guo, Z.M. Qi, T. Shao, Q.P. Wang, H.D. Xie, X. Yao, C.A. Randall, Influence of Ce substitution for Bi in $BiVO_4$ and the impact on the phase evolution and microwave dielectric properties, Inorg. Chem., 53 (2014) 1048-1055.

[23] G.G. Yao, C.J. Pei, P. Liu, J.P. Zhou, H.W. Zhang, Microwave dielectric properties of low temperature sintering $Ca_5Mn_4(VO_4)_6$ ceramics, J. Mater. Sci.: Mater. Electron., 27 (2016) 7292-7296.

[24] C.Z. Yin, C.C. Li, G.J. Yang, L. Fang, Y.H. Yuan, L.L. Shu, J. Khaliq, $NaCa_4V_5O_{17}$: A low-firing microwave dielectric ceramic with low permittivity and chemical compatibility with silver for LTCC applications, J. Eur. Ceram. Soc., 40 (2020) 386-390.

[25] M.T. Paques-Ledent, Double vanadates $LiMgVO_4$, $LiMnVO_4$, $LiCdVO_4$, $NaCdVO_4$ and $NaCaVO_4$: Structure and vibrational spectrum, Chem. Phys. Lett., 35 (1975) 375-378.

[26] P. Biswas, V. Kumar, O.M. Ntwaeaborwa, H.C. Swart, A novel orange-red emitting $NaCaVO_4$: Sm^{3+} phosphor for solid state lighting, Appl. Phys. Lett., 1728 (2016) 020552.

[27] B.V. Slobodin, L.L. Surat, Subsolidus phase relations in the systems M^+O-$M^{2+}O$-V_2O_5 (M^+ = Li, Na, K, Rb, Cs; M^{2+} = Mg, Ca), Inorganic Materials, 40 (2004) 188-194.

[28] B.W. Hakki, P.D. Coleman, A dielectric resonant method of measuring inductive capacitance in the millimeter rage, IEEE Trans Microw Theory Tech 8 (1960) 401-410.

[29] F. Lichtenberg, A. Herrnberger, K. Wiedenmann, Synthesis, structural, magnetic and transport properties of layered perovskite-related titanates, niobates and tantalates of the type $A_nB_nO_{3n+2}$, $A'A_{k-1}B_kO_{3k+1}$ and $A_mB_{m-1}O_{3m}$, Prog. Solid State Chem., 36 (2008) 253-387.

[30] C.C. Li, H.C. Xiang, M.Y. Xu, Y. Tang, L. Fang, Li_2AGeO_4 (A = Zn, Mg): Two novel low-permittivity microwave dielectric ceramics with olivine structure, J. Eur. Ceram. Soc., 35 (2000) 2445-2456.

[31] X.Q. Song, K. Du, J. Li, X.K. Lan, W.Z. Lu, X.H. Wang, W. Lei, Low-fired fluoride microwave dielectric ceramics with low dielectric loss, Ceram. Int., 45 (2019) 279-286.

[32] S.H. Yoon, D.W. Kim, S.Y. Cho, K.S. Hong, Investigation of the relations between structure and microwave dielectric properties of divalent metal tungstate compounds, J. Eur. Ceram. Soc., 26 (2006) 2051-2054.

[33] R.D. Shannon, Dielectric polarizabilities of ions in oxides and fluorides, J. Appl. Phys., 73 (1993) 348-366.

[34] J. Zhang, R.Z. Zuo, Raman scattering and infrared reflectivity study of orthorhombic/ monoclinic $LaTiNbO_6$ microwave dielectric ceramics by A/B-site substitution, Ceram. Int., 44 (2018) 16191-16198.

[35] J. Guo, D. Zhou, L. Wang, H. Wang, T. Shao, Z.M. Qi, X. Yao, Infrared spectra, Raman spectra, microwave dielectric properties and simulation for effective permittivity of temperature stable ceramics $AMoO_4$-TiO_2 (A = Ca, Sr), Dalton Trans., 42 (2013) 1483-1491.

[36] M.T. Paques-Ledent, Isomorphism of HT-$NaCaAsO_4$ and HT-$AgCaAsO_4$: new structural data and vibrational study, J. Inorg. Nucl. Chem., 38 (1976) 215-220.

[37] C. Kai, C.C. Li, H.C. Xiang, Y. Tang, Y.H. Sun, L. Fang, Phase formation and microwave dielectric properties of $BiMVO_5$ (M = Ca, Mg) ceramics potential for low temperature co-fired ceramics application, J. Am. Ceram. Soc., 102 (2019) 362-371.

[38] J.Q. Chen, Y. Tang, H.C. Xiang, L. Fang, H. Porwal, C.C. Li, Microwave dielectric properties and infrared reflectivity spectra analysis of two novel low-firing $AgCa_2B_2V_3O_{12}$ (B = Mg, Zn) ceramics with garnet structure, J. Eur. Ceram. Soc., 38 (2018) 4670-4676.

[39] G. Subodh, M.T. Sebastian, Glass-free $Zn_2Te_3O_8$ microwave ceramic for LTCC applications, J. Am. Ceram. Soc., 90

(2010) 2266-2268.
[40] N.X. Xu, J.H. Zhou, H. Yang, Q.L. Zhang, M.J. Wang, L. Hu, Structural evolution and microwave dielectric properties of MgO-LiF co-doped Li_2TiO_3 ceramics for LTCC applications, Ceram. Int., 40 (2014) 15191-15198.

Table 1 Phonon parameters obtained from the fitting of the infrared reflectivity spectra of $NaCaVO_4$ ceramic

Mode	ω_{oj} (cm^{-1})	ω_{pj} (cm^{-1})	γ_j (cm^{-1})	$\Delta\varepsilon_j$
1	85.88	123.68	2.07	0.335
2	125.49	31.765	0.6641	0.0315
3	193.53	129.27	0.446	0.106
4	242.37	240.07	0.981	0.0885
5	271.76	243.46	0.803	0.198
6	335.92	81.057	0.582	0.0631
7	397.05	135.95	0.717	0.0785
8	546.51	138.62	0.0643	0.21
9	655.37	196.08	0.0895	0.232
10	768.27	448.51	0.341	0.106
11	858.81	99.841	0.0135	0.0368
12	883.95	155.68	0.031	0.0369
13	902.98	146.08	0.0262	0.0285
14	917.32	95.998	0.011	0.0234
$NaCaVO_4$	$\varepsilon_\infty = 1.52$	$\varepsilon_r = 8.34$		

Table 2 Sintering temperature, dielectric properties, and chemical reaction with electrodes of some low-firing vanadates in different structures

Phase	S.T (ºC)	Density (g/cm^3)	ε_r	$Q\times f$ (GHz)	τ_f (ppm/ºC)	electrode	Reference
$SrMgV_2O_7$	780	3.48	16	21,300	-70	Ag	[14]
$NaCa_4V_5O_{17}$	840	3.03	9.72	51,000	-84	Ag	[24]
$BiCaVO_5$	820	5.33	15.7	55,000	-71	Ag	[37]
$BiMgVO_5$	820	5.45	18.55	86,860	-65	Ag	[37]
$AgCa_2Mg_2V_3O_{12}$	750	3.96	23.3	26,900	19.3	Ag	[38]
$AgCa_2Zn_2V_3O_{12}$	750	4.49	26.4	28,400	-18.4	Ag	[38]
$NaCaVO_4$	720	2.87	9.9	31,600	-66.5	Ag	This work

Figure captions:

Figure 1 (a) DSC and TG curves of the raw mixed powders (unfired); (b) X-ray diffraction profiles recorded on the calcined powders at selected temperatures from 640 to 720 ^{o}C; (c) Rietveld refinement on the powder XRD data using Fullprof software; (d) the crystal structure schematic of $NaCaVO_4$;

Figure 2 SEM images of the thermally etched surfaces of the ceramics sintered at (a) 660 ^{o}C, (b) 680 ^{o}C, (c) 700 ^{o}C, (d) 720 ^{o}C, (e) 740 ^{o}C; (f) the bulk density and relative density sintered at various temperatures;

Figure 3 Microwave dielectric properties (ε_r, $Q\times f$, and τ_f) of $NaCaVO_4$ ceramics sintered at various temperatures from 660 to 740 ^{o}C;

Figure 4 (a) The measured and calculated infrared spectra and (b) the real and imaginary parts of the complex responses obtained from the fitting of the IR reflectivity spectra;

Figure 5 (a) XRD and (b) SEM micrograph of $NaCaVO_4$ cofired with the silver electrode at 720 °C (EDS analysis of Ag is shown in the inset).

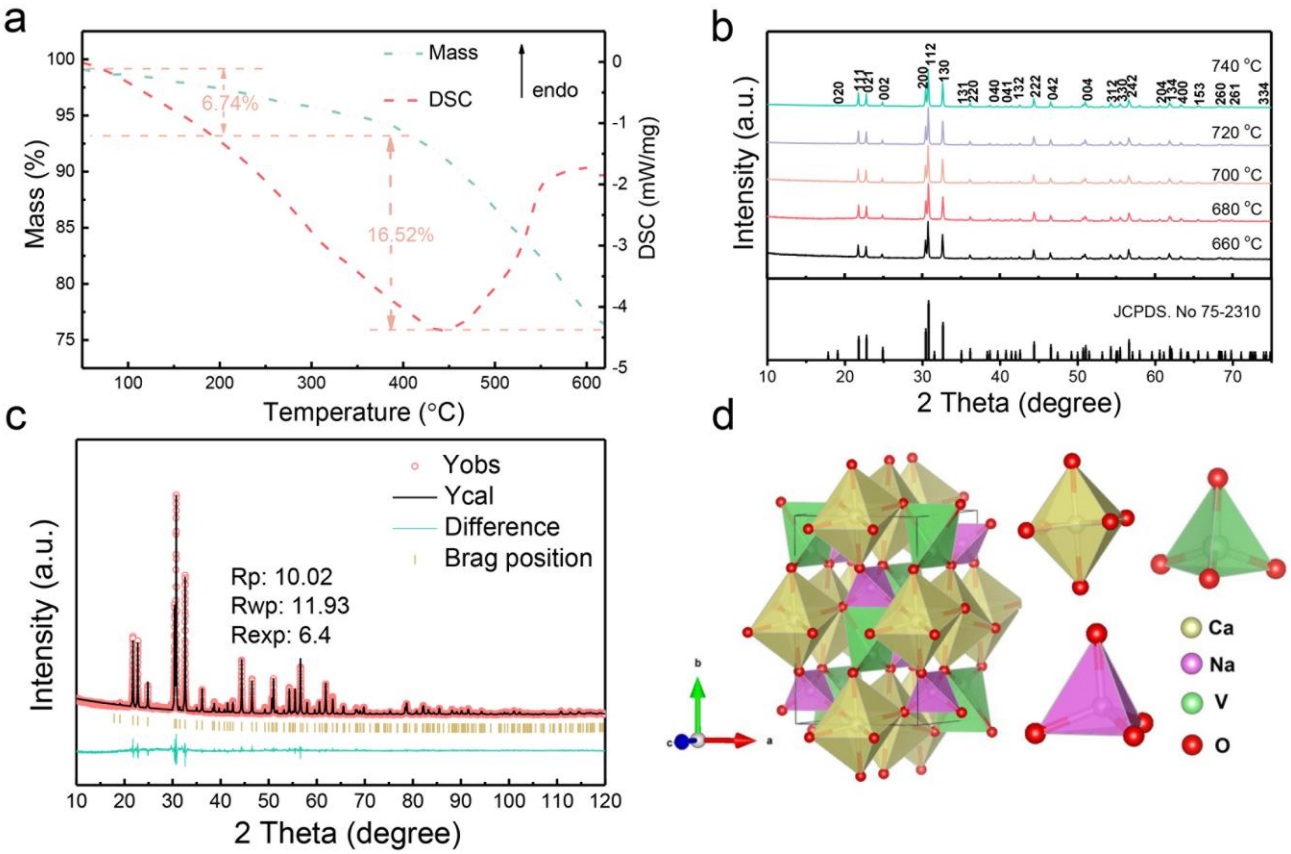
a
Mass
DSC
endo
6.74%
16.52%
Mass (%)
DSC (mW/mg)
Temperature (°C)
b
740 °C
720 °C
700 °C
680 °C
660 °C
JCPDS. No 75-2310
Intensity (a.u.)
2 Theta (degree)
c
Yobs
Ycal
Difference
Brag position
Rp: 10.02
Rwp: 11.93
Rexp: 6.4
Intensity (a.u.)
2 Theta (degree)
d
Ca
Na
V
O

Figure 1

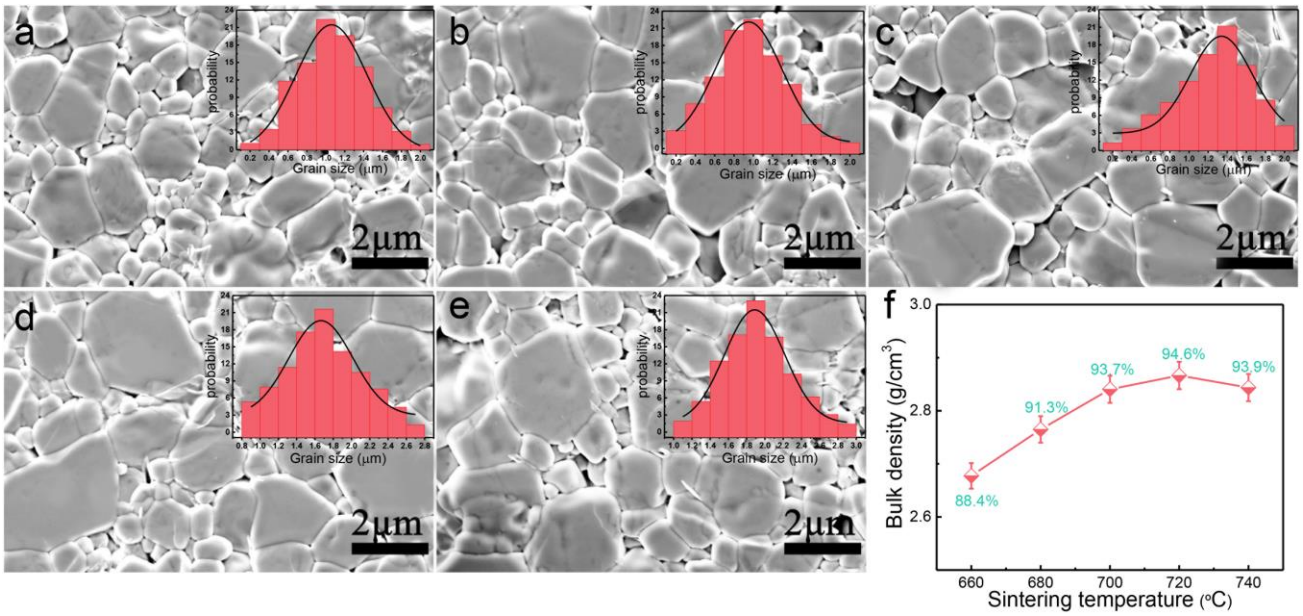
a
b
c
d
e
f
probability
Grain size (μm)
2μm
Bulk density (g/cm^3)
Sintering temperature (°C)
88.4%
91.3%
93.7%
94.6%
93.9%

Figure 2

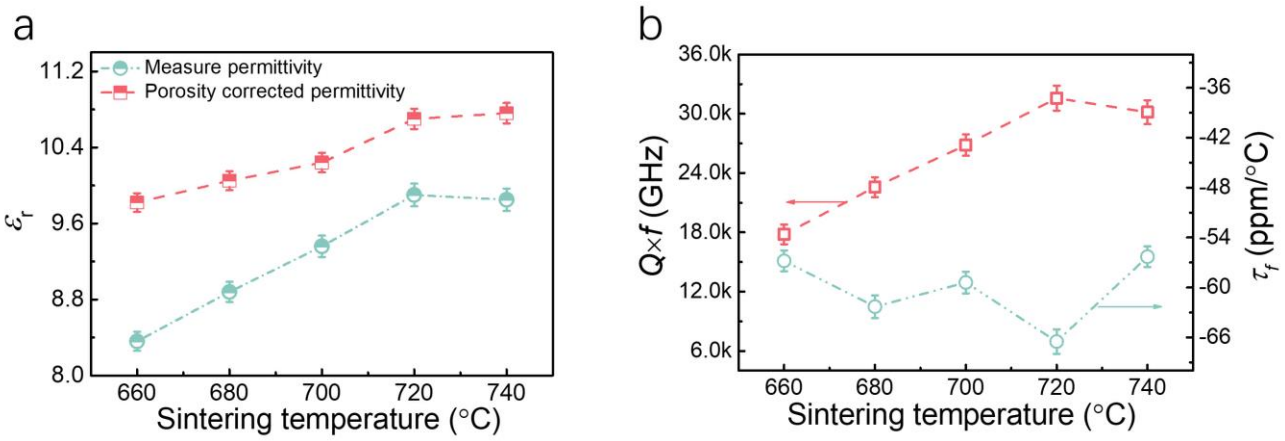
a
Measure permittivity
Porosity corrected permittivity
ε_r
11.2
10.4
9.6
8.8
8.0
660
680
700
720
740
Sintering temperature (°C)
b
36.0k
30.0k
24.0k
18.0k
12.0k
6.0k
Q×f (GHz)
-36
-42
-48
-54
-60
-66
τ_f (ppm/°C)
660
680
700
720
740
Sintering temperature (°C)

Figure 3

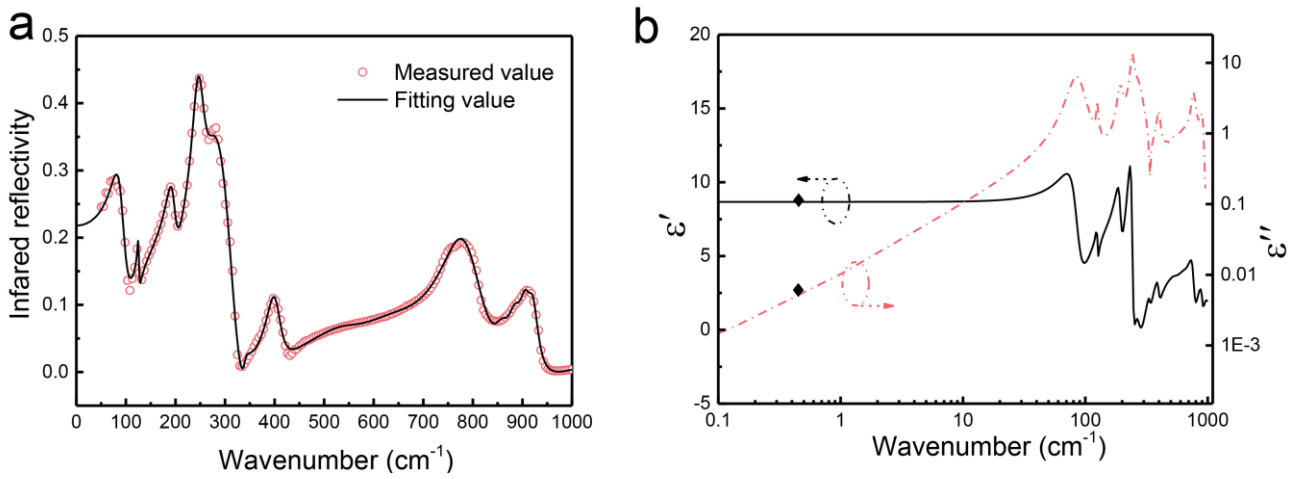
a
Measured value
Fitting value
Infared reflectivity
Wavenumber (cm-1)
b
ε′
ε″
Wavenumber (cm-1)

Figure 4

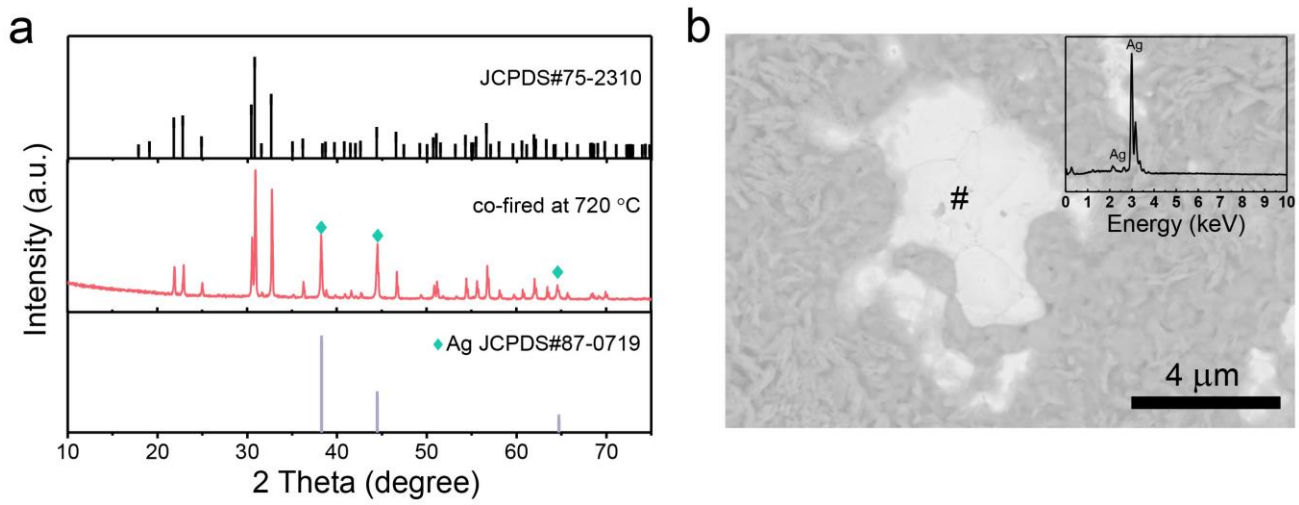
a
JCPDS#75-2310
co-fired at 720 °C
Ag JCPDS#87-0719
Intensity (a.u.)
10 20 30 40 50 60 70
2 Theta (degree)
b
#
Ag
Ag
0 1 2 3 4 5 6 7 8 9 10
Energy (keV)
4 μm

Figure 5